Appearance of a homochiral state of crystals induced by random fluctuation in grinding

Hiroyasu Katsuno[1,*] and Makio Uwaha[2,†]
[1]*Computer Centre, Gakushuin University, 1-5-1 Mejiro, Toshima-ku, Tokyo 171-8588, Japan*
[2]*Department of Physics, Nagoya University, Furo-cho, Chikusa-ku, Nagoya 464-8602, Japan*
(Received 10 September 2012; published 19 November 2012)

We study crystallization of chiral crystals from achiral molecules using a master equation based on a simple reaction model. Although there is no chiral symmetry breaking in the reaction model, random fluctuations drive the system to a homochiral state. The time necessary for the appearance of the homochiral state is proportional to the total number of molecules in the system. This behavior is described by a diffusion equation in a size space with a position-dependent diffusion coefficient. We also study the effect of chiral impurities, which affect the crystal growth. Depending on the type of impurities, the chiral symmetry breaking occurs either deterministically or with the help of random fluctuations.

DOI: 10.1103/PhysRevE.86.051608 PACS number(s): 81.10.Aj, 87.15.Ya, 87.15.nt, 05.10.Gg

I. INTRODUCTION

Achiral molecules of some materials such as $NaClO_3$ and SiO_2 form a pair of chiral crystal structures. Spontaneous symmetry breaking from an achiral solution to chiral crystals occurs microscopically during crystallization, and racemic mixtures of crystals are obtained from a supersaturated solution so that chiral symmetry is macroscopically restored [1]. Macroscopic spontaneous chiral symmetry breaking in crystallization has been found [2,3]. If one makes $NaClO_3$ crystals from a supersaturated solution under stirring, almost all crystals grown from the solution have the same chirality. The chirality of crystals obtained in each experiment is completely random, and the cause of this phenomenon is attributed to secondary nucleation [3–8]. Focusing on the effect of the flow of solution, chiral symmetry breaking is demonstrated in simulations with chaotic flow [9–11]. Recently, Viedma has shown that chirality conversion of crystals occurs in this system [12]. Starting with powder crystals of both chiral types in a solution, grinding and stirring convert the crystals from the racemic state to a homochiral one, which implies that crystals of the minor chirality disappear. Not only has been confirmed the same phenomenon of chirality conversion in another achiral molecular system [13], but also chirality conversion has been found in an organic system (an amino acid derivative) by Noorduin *et al.* [14,15]. In the latter case, a molecule has chirality, which changes in a solution with a base. The conversion from racemic conglomerates to homochiral crystals implies simultaneous conversion of molecular chirality. Such phenomena have been observed in other organic systems [16–18], and the resultant chirality can be controlled with the use of additives [14,19,20]. In order to understand the mechanism of the appearance of the homochiral state (such a process may be called Viedma ripening [15]), several other theoretical models have been proposed [11,21–30]. Some of these models, which include nonlinear effect, reproduce the experimentally observed exponential increase of the enantiomeric excess (EE). With regard to chemical reaction, by Sugimori *et al.* [31], fluctuation is shown to induce a homochiral state in a small system, although the rate equation analysis predicts no chiral symmetry breaking.

In the present paper, following the analysis of Ref. [31], we study the mechanism of the chirality conversion by fluctuation. In Sec. II, the simplest model of crystal growth for chiral crystals with grinding is introduced. The rate equation can describe only the evolution of average values and homochirality does not appear. In order to take account of the effect of fluctuations, we study a stochastic master equation model in Sec. III. With a numerical integration of the master equation for a small system, the change of the probability distribution is studied. A homochiral state is shown to appear temporarily. In Sec. IV, the waiting time for the appearance of the homochiral state is studied using an eigenvalue analysis. Since the master equation is hard to solve numerically for a large system, we performed Monte Carlo simulation of the model in Sec. V. In Sec. VI, we also study the appearance of a homochirality induced by chiral impurities that affect the growth and/or decay rate of crystallization. The results are summarized in Sec. VII.

II. RATE EQUATION APPROACH

We consider the amplification of a chirality imbalance in crystallization of achiral molecules. In the experiments [12–17] of Viedma ripening, the important operation is grinding and stirring. Crystals are distributed uniformly in a solution by stirring, and the size distribution of crystals is steady because of the grinding. Therefore, we may neglect a distribution of clusters in space and size. In this section, we use the simplest reaction model, which includes the processes of the crystal growth and dissolution, using the masses of achiral molecules and chiral crystals.

Our model consists of three components: achiral molecules (Z), and two types of chiral crystals (X and Y). The reaction processes are described as

$$\frac{dz}{dt} = -kz(x+y) + \lambda(x+y), \tag{1}$$

$$\frac{dx}{dt} = kzx - \lambda x, \tag{2}$$

$$\frac{dy}{dt} = kzy - \lambda y, \tag{3}$$

*katsuno@gakushuin.ac.jp
†uwaha@nagoya-u.jp

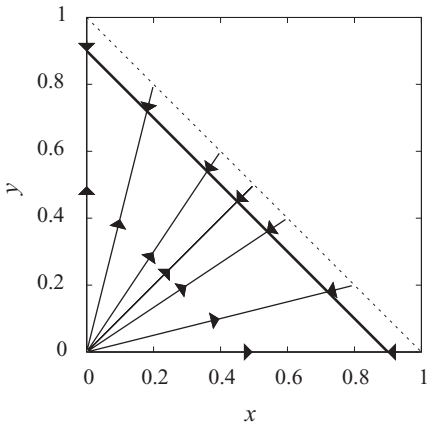

FIG. 1. Flow diagram of Eqs. (2) and (3). The thick solid line, $x + y = 0.9$, represents the fixed line.

where z, x, y are the normalized masses of monomers, crystals X, and crystals Y, respectively. The terms proportional to k represent the growth processes of X and Y with attachment of monomers. The terms proportional to λ represent the decay processes of X and Y by detachment of monomers. The rate equations satisfy the mass conservation condition $z + x + y = 1$.

The analytical solution is

$$x(t) = \frac{(km - \lambda)x_0}{k(x_0 + y_0) + \{k(m - x_0 - y_0) - \lambda\}\exp\{-(km - \lambda)t\}}, \tag{4}$$

$$y(t) = \frac{(km - \lambda)y_0}{k(x_0 + y_0) + \{k(m - x_0 - y_0) - \lambda\}\exp\{-(km - \lambda)t\}}, \tag{5}$$

where x_0 and y_0 represent initial masses of crystals X and Y, respectively. From the solution Eqs. (4) and (5), the ratio $x(t)/y(t)$ is constant in time. By solving $dz/dt = 0$, it is easily seen that any final states are on the fixed line in the x-y plane given by

$$z = \frac{\lambda}{k}, \tag{6}$$

$$x + y = 1 - z, \tag{7}$$

for various initial condition (x_0, y_0) except $x_0 = y_0 = 0$.

The time evolution is depicted as a flow diagram with $\lambda/k = 0.1$ in Fig. 1(a). The thick solid line represents the fixed line $x + y = 1 - \lambda/k = 0.9$. The flow is radial from the origin and the EE, which is defined by $\phi = (x - y)/(x + y)$, does not change with time. Therefore, without fluctuation of the system, any change of chirality is not possible.

III. MASTER EQUATION

In order to study the effect of random fluctuation on the simplest system studied in Sec. II, following Ref. [31], we consider a stochastic model. The total number of molecules is constant $N = N_z + N_x + N_y$, where N_z, N_x and N_y represent the number of single molecules Z, the number of molecules in X and Y, respectively. The system is described by the probability distribution $P(\boldsymbol{X})$ of a state $\boldsymbol{X} = (N_x, N_y)$ (Note that $N_z = N - N_x - N_y$). The growth rate k and the decay rate λ are related to the realization probability of the corresponding processes.

A state $\boldsymbol{X}$ changes to another state $\boldsymbol{X}' = \boldsymbol{X} + \boldsymbol{q}$ with a transition probability $W(\boldsymbol{X}; \boldsymbol{q})$. The probability $P(\boldsymbol{X})$ evolves according to the master equation

$$\frac{\partial P(\boldsymbol{X})}{\partial t} = \sum_{\boldsymbol{q}} W(\boldsymbol{X} - \boldsymbol{q}; \boldsymbol{q})P(\boldsymbol{X} - \boldsymbol{q}) - \sum_{\boldsymbol{q}} W(\boldsymbol{X}; \boldsymbol{q})P(\boldsymbol{X}). \tag{8}$$

The transition probability $W(\boldsymbol{X}; \boldsymbol{q})$ for a change of the state depends on the possible processes in the system. Thus, the transition probabilities are

$$W(\{N_x, N_y\}; \{+1, 0\}) = k'(N - N_x - N_y)N_x, \tag{9}$$

$$W(\{N_x, N_y\}; \{0, +1\}) = k'(N - N_x - N_y)N_y, \tag{10}$$

$$W(\{N_x, N_y\}; \{-1, 0\}) = \lambda N_x, \tag{11}$$

$$W(\{N_x, N_y\}; \{0, -1\}) = \lambda N_y. \tag{12}$$

The growth rate k' is related to the macroscopic reaction rate k as $k' = k/N$. Other transition probabilities $W(\boldsymbol{X}; \boldsymbol{q})$ are zero. The explicit form of the master equation is expressed as

$$\begin{aligned}\frac{\partial P(N_x, N_y)}{\partial t} &= k'(N - N_x - N_y + 1)\{(N_x - 1)P(N_x - 1, N_y) \\ &\quad + (N_y - 1)P(N_x, N_y - 1)\} \\ &\quad + \lambda\{(N_x + 1)P(N_x + 1, N_y) + (N_y + 1)P(N_x, N_y + 1)\} \\ &\quad - \{k'(N - N_x - N_y) + \lambda\}(N_x + N_y)P(N_x, N_y).\end{aligned} \tag{13}$$

A state $\boldsymbol{X} = (N_x, N_y)$ moves to one of the nearest-neighbor states on the two-dimensional lattice shown in Fig. 2. The all monomer state $\boldsymbol{X} = (0, 0)$ is a special state because the transition probabilities to any other states are zero.

Figure 3 shows the time evolution of the probability distribution $P(\boldsymbol{X})$ with $N = 16$. The growth rate k' and the decay rate λ are set to $1/16$ and 0.1, respectively. The initial condition is a supersaturated state $P(1, 1) = 1$ as shown in

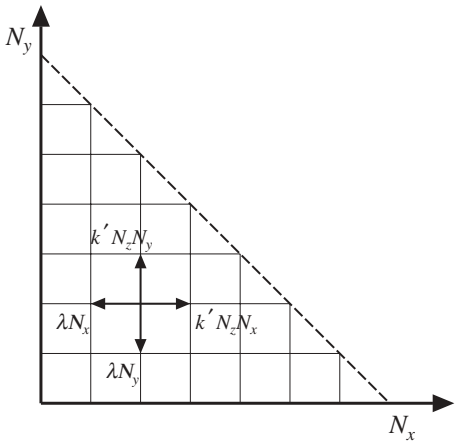

FIG. 2. The schematic figure of the change of a state in the number space. A state moves to one of the nearest-neighbor states.

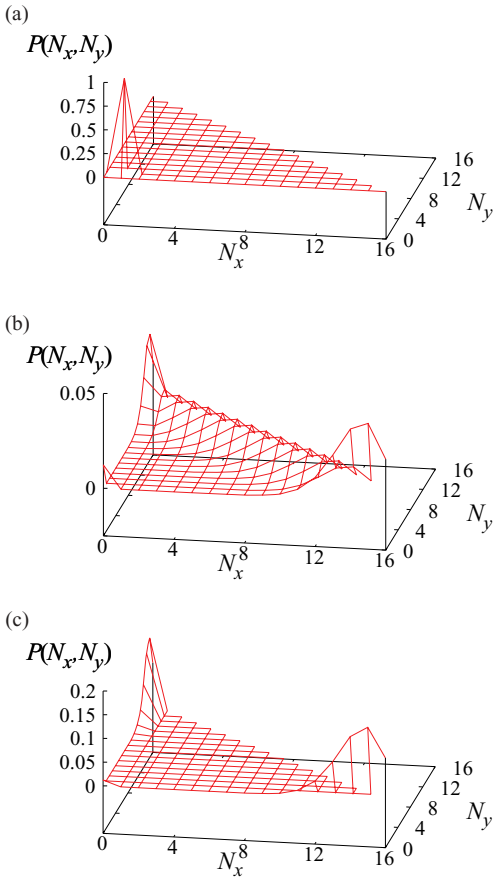

FIG. 3. (Color online) Time evolution of the probability distribution obtained from Eq. (13) with $k = 1$, $\lambda = 0.1$, and $N = 16$. The initial state is $P(1,1) = 1$. The corresponding time is at (a) $t = 0$, (b) $t = 10$, and (c) $t = 1000$.

Fig. 3(a). As shown in Fig. 3(b), the state develops onto the fixed line $N_x + N_y = 14.4 = N_{\rm st}$ obtained from Eq. (7). In Fig. 3(c), the states on the fixed line seem to flow into the chiral states $(N_{\rm st},0)$ or $(0,N_{\rm st})$. The reason is that a state on the fixed line $N_x + N_y = N_{\rm st}$ can change into another state by fluctuation. The probability distribution is always symmetric with regard to the line $N_x = N_y$.

With the use of the probability distribution $P(\boldsymbol{X})$, the expectation value of the absolute enantiomeric excess is easily obtained as

$$\langle|\phi|\rangle = \sum_{N_x,N_y} \left|\frac{N_x - N_y}{N_x + N_y}\right| P(\boldsymbol{X}). \tag{14}$$

The imbalance of the probability distribution is reflected in the magnitude of $\langle|\phi|\rangle$. Figure 4 shows the time evolution of the EE. The average value $\langle\phi\rangle$ is always zero because the initial distribution is symmetric. In Fig. 4(a), $\langle|\phi|\rangle$ increases sharply and linearly until $t \simeq 1$ and increases slowly after $t \sim 4$. The relaxation in $10 < t < 300$ is characterized by the form

$$\langle|\phi|\rangle = 1 - a\exp\left(-\frac{t}{\tau_4}\right), \tag{15}$$

where τ_4 is a characteristic time, and $1/\tau_4 = 0.014$. After a long time, $t > 10^6$, the mass of crystals $N_x + N_y$ decreases slightly because there is a small transition probability to the monomer state $\boldsymbol{X} = (0,0)$. Assuming an exponential decay, the relaxation is characterized by the form

$$\langle|\phi|\rangle = b - c\exp\left(\frac{t}{\tau_2}\right), \tag{16}$$

with $1/\tau_2 \sim 10^{-10}$. These values will be discussed later.

The expected final state is $\boldsymbol{X} = (0,0)$ since there is no way to escape from this state, and the probability to fall into this state is finite. However, the numerical result for the small decay rate of the chiral states suggests that the relaxation time to the final state is extremely long and practically infinity (see Sec. IV).

IV. EIGENVALUE ANALYSIS

In the numerical integration of the master equation, the system did not reach the final state and stayed at the temporal symmetric state with two peaks. We analyze the problem in terms of the evolution matrix of the master equation [31]. Since the master equation is a linear equation for the probability distribution, the time evolution is written as

$$\frac{dP(\boldsymbol{X})}{dt} = \sum_{\boldsymbol{X}'} (\boldsymbol{X}|\boldsymbol{M}|\boldsymbol{X}')P(\boldsymbol{X}'), \tag{17}$$

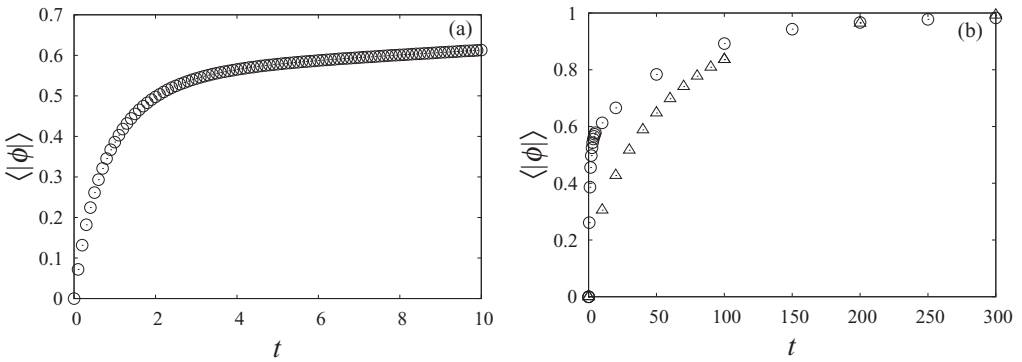

FIG. 4. Time evolution of the average of the absolute value EE. (a) Initial change from the supersaturated condition $P(1,1) = 1$. (b) Change from the initial condition. ◯: $P(1,1) = 1$, △: $P(7,7) = 1$.

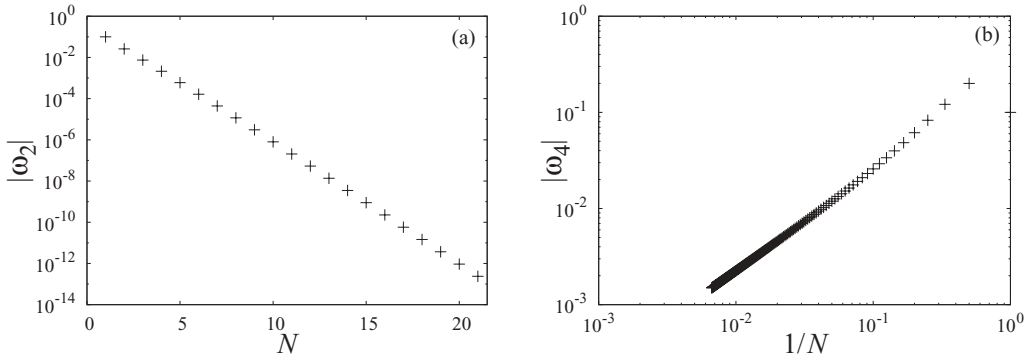

FIG. 5. The size dependence of eigenvalues. (a): The second (and the third) eigenvalue and (b): the fourth eigenvalue.

where the elements of the evolution matrix $\boldsymbol{M}$ are related to the transition probability $W(\boldsymbol{X},\boldsymbol{q})$ as

$$(\boldsymbol{X}|\boldsymbol{M}|\boldsymbol{X}') = \begin{cases} W(\boldsymbol{X}';\boldsymbol{X}-\boldsymbol{X}') & \text{for} \quad \boldsymbol{X}' \neq \boldsymbol{X}, \\ -\sum_{\boldsymbol{q}} W(\boldsymbol{X};\boldsymbol{q}) & \text{for} \quad \boldsymbol{X}' = \boldsymbol{X}. \end{cases}$$

Equation (17) is an eigenvalue equation if we assume the form $P(\boldsymbol{X},t) = P(\boldsymbol{X})e^{\omega t}$. By solving the equation we obtain the decay rate of a distribution of the eigenstate. The largest eigenvalue ω_1 is obviously zero with the eigenvector $P(\boldsymbol{X}) = \delta_{\boldsymbol{X},\boldsymbol{0}}$. The all monomer state $\boldsymbol{X} = (0,0)$ can not decay to any other states. The ith eigenvalues ω_i can be obtained numerically, and they are nonpositive. Their values are related to the decay time τ_i: $\omega_i = -1/\tau_i$.

The second eigenstate and the third eigenstate are degenerate and completely homochiral: $N_x = 0$ or $N_y = 0$. The magnitude $|\omega_2|$ is very small and decreases exponentially with the total number N as shown in Fig. 5(a). The fourth eigenstate is symmetric and its components are nonzero around the fixed line like the distribution shown in Fig. 3(b). The magnitude $|\omega_4|$ decreases with the system size as $1/N$. These eigenvalues correspond to the relaxation times found in the numerical integration of the master equation. For $N = 16$, ω_2 is obtained as -2.3×10^{-10}, which is of the order of the inverse relaxation time $-1/\tau_2 \sim 10^{-10}$ obtained from the integration up to $t \sim 10^{10}$. The fourth eigenvalue ω_4 is about -0.015, which is in good agreement with the inverse relaxation time $-1/\tau_4 = -0.014$.

The relaxation time τ_2 is much longer than τ_4 for any system size, and corresponds to the change from the degenerate state to the all monomer state. It is so long that the all monomer state does not appear in the numerical integration within the limited time.

V. MONTE CARLO SIMULATION OF THE MASTER EQUATION

From the result of Secs. III and IV, the distribution changes as follows: it initially approaches the fixed line obtained from the rate equations, and stays at the points around $\boldsymbol{X} = (N_{\rm st},0)$ or $\boldsymbol{X} = (0,N_{\rm st})$. Finally, the monomer state appears after a long time. In this section, we focus on the appearance of homochiral states and its mechanism. The time development of the system can be regarded as a random walk on the two-dimensional lattice with the transition probability $W(\boldsymbol{X},\boldsymbol{q})$. Instead of solving Eq. (17) we perform a Monte Carlo simulation in which a walker moves to one of the neighboring sites until it arrives at one of the homochiral states: $(N_{\rm st},0)$ and $(0,N_{\rm st})$.

Figure 6(a) shows the change of EE for one sample with the total number $N = 100, 1000, 10000$. The EE seems to increase linearly although its value fluctuates from the initial value $\phi = 0.05$. On average the walker moves from the initial state to the fixed line and it fluctuates around the fixed line. As a result of random walk, the walker finally falls into one of the homochiral states. We define the conversion time τ_f as the time necessary for the completion of homochirality. The conversion time averaged over 100 samples is plotted in Figs. 6(b) and 6(c) for various system size N. The error bars represent the root-mean-square of the data. The conversion time increases linearly with the total number N, and corresponds to the decay time τ_4 from the fixed line state to the homochiral state shown in Fig. 5(b).

The conversion time may be estimated as the following way. A walker arrives at the fixed line deterministically and quickly according to the rate equation. It takes long that a walker moves from a point on the fixed line to the homochiral state $[(N_{\rm st},0)$ or $(0,N_{\rm st})]$. To estimate the conversion time, we suppose that the walker moves only on the fixed line $(N_x, N_{\rm st} - N_x)$ and their neighboring sites $(N_x, N_{\rm st} - N_x \pm 1)$ or $(N_x \pm 1, N_{\rm st} - N_x)$, where $N_{\rm st}$ is assumed to be an integer. The move occurs at the rate given by Eqs. (9)–(12) in a period of time Δt, which we set $1/\lambda N_{\rm st}$. A walker reaches from a site to its neighboring site by one growth process and one decay process of crystals in time $2\Delta t$. The transition probability from $(N_x, N_{\rm st} - N_x)$ to $(N_x + 1, N_{\rm st} - N_x - 1)$ is $N_x(N_{\rm st} - N_x)/N_{\rm st}^2$, where the number of monomers is assumed to be constant. The average displacement and the dispersion of N_x at a certain site are $\langle \Delta N_x \rangle = 0$ and $\langle (\Delta N_x)^2 \rangle = 2N_x(N_{\rm st} - N_x)/{N_{\rm st}}^2$, respectively. We obtain

$$\langle \Delta x' \rangle = 0, \tag{18}$$

$$\langle (\Delta x')^2 \rangle = \frac{2}{N_{\rm st}^2} x'(1-x'), \tag{19}$$

where $x' = N_x/N_{\rm st}$. Therefore the behavior of the walker along the fixed line is described by a diffusion equation with the position-dependent diffusion coefficient $D(x') = \frac{\lambda}{2N_{\rm st}} x'(1 - x')$. This simplified model corresponds to the diffusion process approximation of the Wright-Fisher model studied in the field

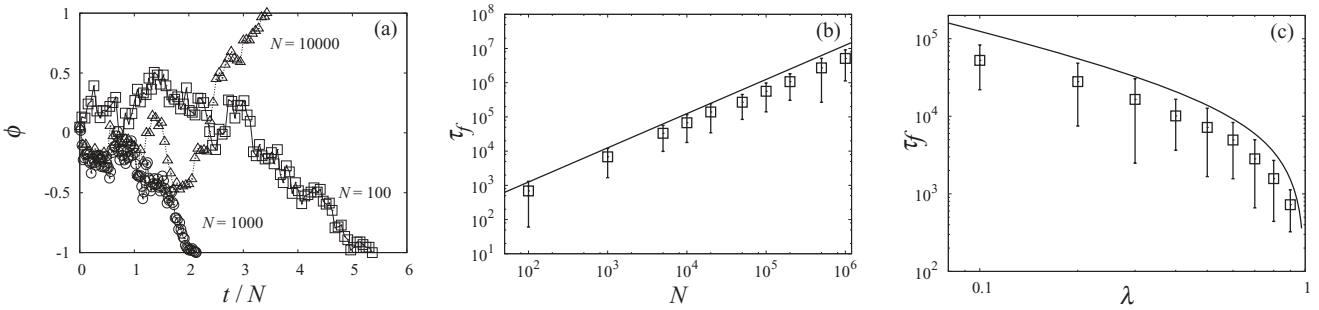

FIG. 6. (a) Time evolution of ϕ in the Monte Carlo simulation. (b) The conversion time for various system size N. (c) The conversion time for various decay rate λ. The solid lines represent the estimated conversion time using the the simplified model Eq. (20).

of population genetics [32,33]. It is known that starting from $x' = x'_0$, a walker reaches $x' = 1$, and the average time is $T = -2(N_{\rm st}/\lambda)(1-x'_0)/x'_0 \times \ln(1-x'_0)$. As the conversion time τ_f is the average time for the walker to reach $x' = 1$ or $x' = 0$, the conversion time τ_f from the initial position x'_0 on the fixed line can be estimated as

$$\begin{aligned}\tau_f &= -\frac{2N_{\rm st}}{\lambda}\{x'_0 \ln x'_0 + (1-x'_0)\ln(1-x'_0)\} \\ &= -\frac{2N}{\lambda}\left\{x_0 \ln\frac{x_0}{1-\lambda/k} + \left(1-\frac{\lambda}{k}-x_0\right)\right. \\ &\quad \left.\times \ln\frac{1-\lambda/k-x_0}{1-\lambda/k}\right\}. \end{aligned} \tag{20}$$

The result is shown as the solid line in Figs. 6(b) and 6(c). Parameters are set as $k = 1$, $\lambda = 0.1$, and $x_0 = 0.45$ in Fig. 6(b), and $k = 1$, $x_0 = (1-\lambda/k)/2$ and $N = 10000$ in Fig. 6(c). The estimation of the conversion time Eq. (20) is in agreement with the simulation results.

VI. IMPURITY EFFECT

In experiment, the chirality of crystals can be controlled by adding chiral impurities [14,19,20], radiating circularly polarized light [34], and changing order of process steps [35]. Since all these effects are attributed to the effect of chiral impurities, we here study the effect of impurities on our model. It is commonly accepted that chiral impurities adsorb onto the crystal surface in a solution and affect the crystal growth of one type of chiral crystals. We consider two types of impurities: one prevents the crystal growth process and the other prevents both growth and decay processes in the same ratio.

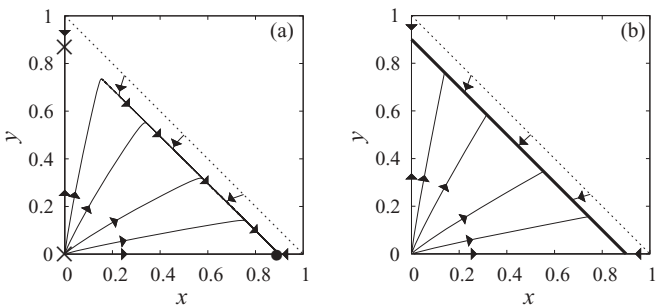

FIG. 7. Flow diagram of (a) Eq. (21) and of (b) Eq. (22). Solid bold line represents the fixed line.

The first type is described in the simple rate equation model by introducing a reduction factor $\alpha(<1)$

$$\begin{aligned}\frac{dx}{dt} &= kzx - \lambda x, \\ \frac{dy}{dt} &= \alpha kzy - \lambda y, \\ z &= 1-x-y. \end{aligned} \tag{21}$$

The second type is described with another reduction factor $\beta(<1)$ as

$$\begin{aligned}\frac{dx}{dt} &= kzx - \lambda x, \\ \frac{dy}{dt} &= \beta kzy - \beta\lambda y, \\ z &= 1-x-y. \end{aligned} \tag{22}$$

Flow diagrams of Eqs. (21) and (22) are shown in Figs. 7(a) with $\alpha = 0.9$ and 7(b) with $\beta = 0.9$, respectively. As $\alpha < 1$ and $\beta < 1$, the ratio x/y increases in the supersaturated condition and decreases in the under saturated condition in the initial time evolution. For the first type [Fig. 7(a)], there are two unstable fixed points and one stable fixed point. Since the mass of monomers at equilibrium for crystal X is lower than that for crystal Y, any initial state with finite x and y reaches the stable homochiral state deterministically. For the second type [Fig. 7(b)], a fixed line appears as in Fig. 1. This type does not change the mass of monomers at equilibrium for both crystals X and Y. As the flow lines are curved as shown in Fig. 7(b), the relative ratio of X increases until the system reaches the fixed line. When the system reaches a state on the fixed line, it is on the state closer to the point $(x^{\rm st},0)$ than in the case of Fig. 1. Then, the fluctuation drives the system along the fixed line to homochirality as in the case of Sec. V with the smaller diffusion coefficient $\beta D(x')$.

VII. SUMMARY

We studied the possibility of the chirality conversion by random fluctuation. We introduced the simple rate equation model of crystallization with grinding of chiral crystals. Our model does not include any effects of convection [10,11] and nonlinearity [21,22,24,29]. The analytical solution shows that the ratio of crystal X and Y does not change. The master equation based on the rate equation was also introduced. According to the numerical integration, the distribution function evolves

from the initial state to the point on the fixed line after about a time $1/\lambda$. The expectation value of the absolute value of the EE $\langle|\phi|\rangle$ increases linearly with time and a steady state appears. We also performed the eigenvalue analysis. The eigenvalue ω_1 of the all monomer state vanishes. The eigenvalues ω_2 and ω_3 of homochiral states decrease exponentially with the system size N, which implies they are practically zero. The eigenvalue ω_4 of the state along the fixed line decreases as $1/N$. The magnitudes of ω_2 and ω_4 are of the order of those obtained by the direct numerical integration.

We performed the Monte Carlo simulation of the stochastic model. The simulation data show that the conversion time increases linearly with the system size. Such a behavior is derived mathematically in a simplified random walker model. Thus, the direct integration of the master equation, the eigenvalue analysis, and the Monte Carlo simulation all show that the conversion of the chirality due to fluctuation is possible but requires a conversion time proportional to the system size.

In the simulation with convective flow [11], the increase in EE seems linear and was attributed to a random selection effect. Also, in our previous work [26], a linear amplification of EE has been observed in a monomer reaction model. Although the model of this paper differs from that of Refs. [11] and [26], we think that homochirality is realized by simple fluctuation without nonlinearity and a similar behavior is expected in such systems. In experiment, in most cases the observed EE changes exponentially in time, and nonlinearity such as cluster growth certainly plays an essential role in the chirality conversion. In some cases, however, a linear change of the EE has been reported [18]. Fluctuation in the atomic scale is not able to produce a homochiral state since $\tau_f \sim N$, but some fluctuation at a different level may play a role.

Effects of chiral impurities added to the system are also discussed. When the impurity differentiates equilibrium mass of monomers for crystals X and Y, homochiral state is realized deterministically. When the impurity does not shift the equilibrium mass of monomers of both, complete homochiral state can be realized only by random fluctuation.

ACKNOWLEDGMENT

The present research is supported by the Japan Society for the Promotion of Science through a Grant-in-Aid.

[1] F. S. Kipping and W. J. Pope, J. Chem. Soc. Trans. **73**, 606 (1898).
[2] D. K. Kondepudi, R. Kaufman, and N. Singh, Science **250**, 975 (1990).
[3] For a review: D. K. Kondepudi and K. Asakura, Acc. Chem. Res. **34**, 946 (2001).
[4] J. M. McBride and R. L. Carter, Angew. Chem., Int. Ed. Engl. **30**, 293 (1991).
[5] B. Martin, A. Tharrington, and X.-l. Wu, Phys. Rev. Lett. **77**, 2826 (1996).
[6] R.-U. Qian and G. D. Botsaris, Chem. Eng. Sci. **53**, 1745 (1998).
[7] T. Buhse, D. Durand, D. Kondepudi, J. Laudadio, and S. Spilker, Phys. Rev. Lett. **84**, 4405 (2000).
[8] Y. Song, W. Chen, and X. Chen, Cryst. Growth Des. **8**, 1448 (2008).
[9] G. Metcalfe and J. M. Ottino, Phys. Rev. Lett. **72**, 2875 (1994).
[10] J. H. E. Cartwright, J. M. García-Ruiz, O. Piro, C. I. Sainz-Díaz, and I. Tuval, Phys. Rev. Lett. **93**, 035502 (2004).
[11] J. H. E. Cartwright, O. Piro, and I. Tuval, Phys. Rev. Lett. **98**, 165501 (2007).
[12] C. Viedma, Phys. Rev. Lett. **94**, 065504 (2005).
[13] P. S. M. Cheung, J. Gagnon, J. Surprenant, Y. Tao, H. Xu, and L. A. Cuccia, Chem. Commun. 987 (2008).
[14] W. L. Noorduin, T. Izumi, A. Millemaggi, M. Leeman, H. Meekes, W. J. P. Van Enckevort, R. M. Kellogg, B. Kaptein, E. Vlieg, and D. G. Blackmond, J. Am. Chem. Soc. **130**, 1158 (2008).
[15] For a review: W. L. Noorduin, E. Vlieg, R. M. Kellogg, and B. Kaptein, Angew. Chem. Int. Ed. **48**, 9600 (2009).
[16] B. Kaptein, W. L. Noorduin, H. Meekes, W. J. P. van Enckevort, R. M. Kellogg, and E. Vlieg, Angew. Chem. Int. Ed. **47**, 1 (2008).
[17] C. Viedma, J. E. Ortiz, T. de Torres, T. Izumi, and D. G. Blackmond, J. Am. Chem. Soc. **130**, 15274 (2008).
[18] S. B. Tsogoeva, S. Wei, M. Freund, and Michael Mauksch, Angew. Chem. Int. Ed. **48**, 590 (2009).
[19] P. S. M. Cheung and L. A. Cuccia, Chem. Commun. 1337 (2009).
[20] W. L. Noorduin, P. van der Asdonk, H. Meekes, W. J. P. van Enckevort, B. Kaptein, M. Leeman, R. M. Kellogg, and E. Vlieg, Angew. Chem. Int. Ed. **48**, 3278 (2009).
[21] M. Uwaha, J. Phys. Soc. Jpn. **73**, 2601 (2004); **77**, 083802 (2008).
[22] J. A. D. Wattis and P. V. Coveney, Org. Life Evol. Biosph. **35**, 243 (2004).
[23] W. L. Noorduin, H. Meekes, A. A. C. Bode, W. J. P. van Enckevort, B. Kaptein, R. M. Kellogg, and E. Vlieg, Cryst. Growth Des. **8**, 1675 (2008).
[24] Y. Saito and H. Hyuga, J. Phys. Soc. Jpn. **77**, 113001 (2008).
[25] M. Uwaha and H. Katsuno, J. Phys. Soc. Jpn. **78**, 023601 (2009).
[26] H. Katsuno and M. Uwaha, J. Cryst. Growth **311**, 4265 (2009).
[27] Y. Saito and H. Hyuga, J. Phys. Soc. Jpn. **78**, 104001 (2009).
[28] M. Uwaha, J. Cryst. Growth **318**, 89 (2011).
[29] Y. Saito and H. Hyuga, J. Cryst. Growth **318**, 93 (2011).
[30] M. Iggland and M. Mazzotti, Cryst. Growth Des. **11**, 4611 (2011).
[31] T. Sugimori, H. Hyuga, and Y. Saito, J. Phys. Soc. Jpn. **77**, 064606 (2008).
[32] M. Kimura and T. Ohta, Genetics **61**, 763 (1969), http://www.ncbi.nlm.nih.gov/pmc/articles/PMC1212239/.
[33] H. Matsuda and K. Ishii, *Mathematics of Genetic Population and Evolution* (Iwanami, Tokyo, 1980) (in Japanese).
[34] W. L. Noorduin *et al.*, Nature Chem. **1**, 729 (2009).
[35] W. L. Noorduin H. Meeks, W. J. P. van Enckevort, B. Kaptein, R. M. Kellogg, and E. Vlieg, Angew. Chem. Int. Ed. **49**, 2539 (2010).